frontiers in Earth Science

ORIGINAL RESEARCH
published: 23 June 2020
doi: 10.3389/feart.2020.00170

Distribution and Eruptive Volume of Aso-4 Pyroclastic Density Current and Tephra Fall Deposits, Japan: A M8 Super-Eruption

Shinji Takarada and Hideo Hoshizumi*

Geological Survey of Japan, National Institute of Advanced Industrial Science and Technology (AIST), Tsukuba, Japan

Estimations of the distribution and eruptive volume of large-scale pyroclastic density current (PDCs) and tephra fall deposits are essential for evaluation of the affected area, long-term volcanic hazards assessments, volcanic activity, and geophysical and petrological quantitative analysis at caldera volcanoes. For this study, the original distributions and eruptive volumes of large-scale PDC (up to 166 km runout distance) and tephra fall deposits derived from the last 87–89 ka caldera-forming eruption (named Aso-4) of Aso volcano in Japan were reevaluated. The original distributions and volumes of PDC deposits just after the eruption were estimated using 3,600 data from geological maps, published research papers, and borehole thickness. The original distributions and volumes of tephra falls were estimated from new isopach maps based on thickness and distribution data of submarine, lacustrine, and subaerial tephra fall deposits. The estimated original volume of the Aso-4 PDC deposits is 340–935 km^3 (5.6–14.8 $\times$ 10^{14} kg). The estimated original volume of the Aso-4 tephra fall deposit is 590–920 km^3 (6.0–9.3 $\times$ 10^{14} kg). The total eruptive volume of the Aso-4 eruption was 930–1,860 km^3 (1.2–2.4 $\times$ 10^{15} kg). This estimation result is about 1.5 to 3 times larger than the previous estimation (>600 km^3). Thus, the Aso-4 eruption is now defined as a M8.1–8.4 (VEI8) super-eruption. The Aso-4 results to be the largest eruption in Japan and the 2nd largest eruption in the world (after the 74 ka Toba eruption) in the last 100 ka.

Keywords: Aso caldera, ignimbrite, co-ignimbrite ash, large-scale eruption, estimation uncertainty, volcanic hazard assessment

OPEN ACCESS

Edited by:
Andrea Bevilacqua, National Institute of Geophysics and Volcanology, Italy

Reviewed by:
Antonio Costa, National Institute of Geophysics and Volcanology, Italy
Greg A. Valentine, University at Buffalo, United States

****Correspondence:***
Shinji Takarada
s-takarada@aist.go.jp

Specialty section:
This article was submitted to Volcanology, a section of the journal Frontiers in Earth Science

Received: *06 April 2020*
Accepted: *04 May 2020*
Published: *23 June 2020*

Citation:
Takarada S and Hoshizumi H (2020) Distribution and Eruptive Volume of Aso-4 Pyroclastic Density Current and Tephra Fall Deposits, Japan: A M8 Super-Eruption. Front. Earth Sci. 8:170. doi: 10.3389/feart.2020.00170

INTRODUCTION

Accurate determinations of the eruptive volumes of large-scale caldera-forming eruptions provide an essential parameter for assessing long-term eruption records, eruption activity evaluations, and quantitative geophysical and petrological investigations. The eruptive volume is also used for developing reliable volume vs. time diagrams and volcanic hazard assessments. Recently, several studies to estimate the eruptive volume of tephra falls derived from large-scale volcanic eruptions were made (e.g., Costa et al., 2014; Kandlbauer and Sparks, 2014). Furthermore, a large number of studies have been published to estimate the eruptive volume of tephra fall deposits (e.g., Pyle, 1989, 1995; Fierstein and Nathenson, 1992; Legros, 2000; Bonadonna and Houghton, 2005;

Sulpizio, 2005; Bonadonna and Costa, 2012; Engwell et al., 2013). However, relatively few studies have reported high-resolution eruptive volume estimates of large-scale caldera-forming pyroclastic density current (PDC) deposits (e.g., Cook et al., 2016).

The 87–89 ka Aso-4 eruption is the largest of the 4 major caldera-forming eruptions from Aso caldera. It is also considered to be one of the largest eruptions in Japan in the last 1 Ma (e.g., Hayakawa, 1995). Here we estimated the original distributions and eruptive volume of the large-scale Aso-4 PDC deposit, based on more than 3,600 boreholes, topography, and outcrop data with a 7 km × 5.5 km mesh interval. The eruptive volume of the co-ignimbrite ash fall deposit derived from the Aso-4 eruption was also estimated using new isopach maps based on thickness data from about 70 locations, including submarine and lacustrine sample data.

GEOLOGY OF ASO-4 PDC DEPOSITS

Aso caldera, 25 km N-S × 18 km E-W, is located in central Kyushu and is one of the largest calderas in Japan (Ono et al., 1977; Ono and Watanabe, 1985). It was formed by four major eruptive events that produced widespread PDC deposits: Aso-1 (ca. 270 ka), Aso-2 (ca. 140 ka), Aso-3 (ca. 120 ka), and Aso-4 (89 ka) PDCs (Ono and Watanabe, 1985; K-Ar ages from Matsumoto et al., 1991). The Aso-4 PDC deposit records the largest eruptive event and is widely distributed in northern and central Kyushu and western Yamaguchi Prefecture (**Figure 1**). The Aso-4 PDCs reached as far as 166 km to NNE from the central caldera (**Figure 1**), one of the largest runout distances ever recorded. For comparison, the runout distances of the 18.8 Ma Peach Spring Tuff, United States, reached as far as 175 km (Roche et al., 2016), the 40 Ma Big Cottonwood Canyon Tuff, United States, reached >150 km (Henry, 2008), and the 186 AD Taupo ignimbrite, New Zealand, reached ca. 80 km (Wilson and Walker, 1985). A large number of studies were made on the Aso-4 PDC deposits such as Ono (1965), Watanabe and Ono (1969), Watanabe (1972, 1978, 1979), Ono et al. (1977), Ono and Watanabe (1983, 1985), Hoshizumi et al. (1988), Suzuki-Kamata and Kamata (1990), Kamata (1997), Saito et al. (2005), and Okumura et al. (2010). Ono and Watanabe (1983) defined the approximate distributions of Aso-1, Aso-2, Aso-3, and Aso-4 PDC deposits. The Aso-1 and Aso-2 PDC deposits are distributed as far as 30 km from the caldera, Aso-3 PDC deposit is distributed as far as 50 km W and 70 km E from the caldera and Aso-4 PDC deposit is distributed widely and as far as 166 km NNE (**Figure 1**; the distribution and volume of the Aso-4 PDC deposits are examined in this study). The distal facies of the Aso-4 PDC deposits in Yamaguchi Prefecture were studied by Matsuo and Takahashi (1974), Matsuo (1978, 1984, 2001), and Matsuo and Kawaguchi (2015). The Aso-4 PDC deposit contains hornblende phenocrysts, which is a marker to distinguish it from the Aso-1, 2, and 3 PDC deposits (e.g., Ono et al., 1977; Ono and Watanabe, 1985; Saito et al., 2005). The Aso-4 PDC deposits within terrace deposits in Miyazaki and Fukuoka Prefectures were reported by Nagaoka (1984), Shimoyama et al. (1984), and Endo and Suzuki (1986).

Aso-4 tephra fall deposits are widely distributed and are one of the most significant marker tephras for volcanological studies throughout Japan (Machida et al., 1985; Machida and Arai, 1988, 2003; Nagahashi et al., 2004, 2007; Aoki, 2008; Tsuji et al., 2018). No preceding Plinian tephra fall deposits have been observed beneath the Aso-4 PDC deposits (Ono et al., 1977; Ono and Watanabe, 1983), suggesting most of the widely distributed tephra fall deposits are derived from the co-ignimbrite ash (Machida et al., 1985; Machida and Arai, 2003). The thickness of the Aso-4 tephra fall deposits is a few cm in Omachi City, Nagano Prefecture, 5 cm in Noshiro City, Akita Prefecture, and 15 cm in Abashiri City, Hokkaido (**Figure 1**; Machida et al., 1985).

The Aso-4 PDC deposits consist of several massive dacite units, which are defined by lithology, facies, and cooling history (e.g., Watanabe, 1978; Hoshizumi et al., 1988; Kamata, 1997). Aso-4A and 4B units were defined by Ono and Soya (1968) and Ono et al. (1977). Aso-4A, Aso-4T, and Aso-4B units were subsequently defined by Hoshizumi et al. (1988) and Kamata (1997) (**Figure 2**). More detailed subdivisions comprise the Oyatsu white pumice flow, Koei ash flow, Hatobira pumice flow, Yame pumice flow, Motoigi gray pumice flow, Benri scoria flow, Tosu orange pumice flow, and Kunomine scoria flow deposits, which were defined by Watanabe (1978) in the western part of the Aso caldera area. The Tosu orange pumice flow (Aso-4T) is a low-aspect ratio ignimbrite, which shows widely distributed ignimbrite-veneer type deposits (Watanabe, 1978; Suzuki-Kamata and Kamata, 1990).

The Aso-4A PDC deposits consist of <100 m-thick, densely to partially welded and non-welded, poorly sorted, and massive ignimbrite containing relatively large amounts of pumice lapilli and blocks (**Figures 2**, **3a**,**b**). The Aso-4A PDC deposits are normally massive, but flow unit boundaries are sometimes observed in a few-meters interval, suggesting that this consists of >10–20 flow units. The upper non-welded facies are sometimes eroded. The lower part of the ignimbrite consists of non-welded grayish white to gray-colored matrix and pumice block and lapilli. The layer 2a (Sparks et al., 1973) is sometimes developed at the base of the non-welded facies. Breccia facies are sometimes developed at the bottom of the Aso-4A PDC deposit (**Figures 2**, **3a**). The breccia facies consist of lithic-rich matrix and boulders, blocks, and lapilli-size dense rocks with a small amount of pumice lapilli. Tuff breccia blocks and boulders are sometimes included in the breccia facies. The densely welded facies consist of a dark gray matrix and black fiamme-rich block and lapilli (**Figures 2**, **3d**). The size of the fiamme is >5 cm (sometimes >20–50 cm). A devitrification zone is developed at the lower part of the welded facies. The partially welded facies consist of gray to dark gray matrix and grayish white flattened pumice blocks and lapilli (**Figure 2**). The welded facies show 1–2 m wide columnar joints (**Figure 3c**). The non-welded facies consist of a grayish white to gray matrix and 15–40 vol. % of pumice blocks and lapilli (**Figures 2**, **3b**). The pumice blocks and lapilli are gray to white with tube-type vesicles and are usually <20 cm in size. The matrix consists of fine glassy ash and <4 mm-size crystal fragments. The Aso-4A PDC deposits are the

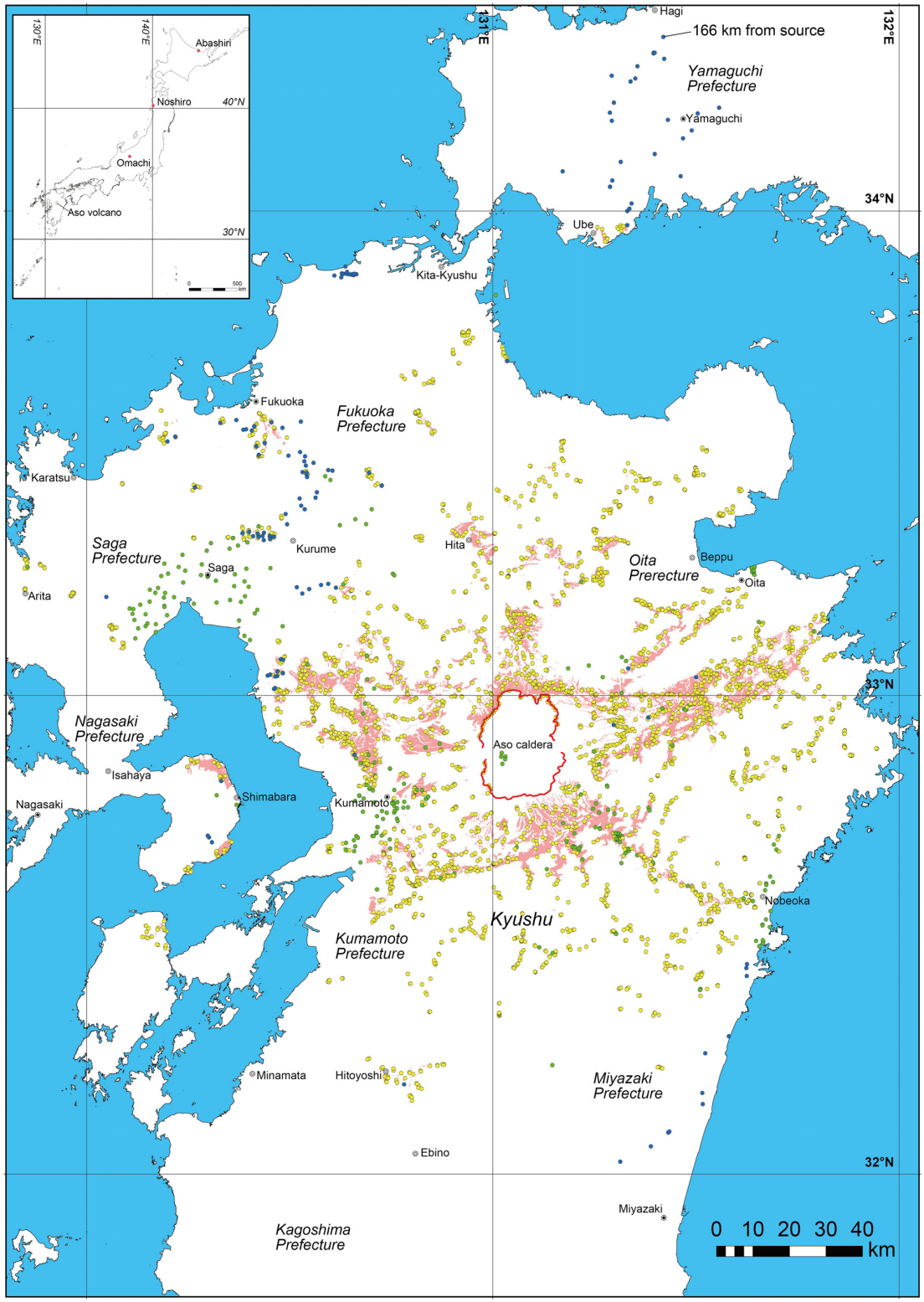

FIGURE 1 | Distribution of current Aso-4 PDC deposit exposures (orange-colored part) and Aso caldera (red line). Circles on the map indicate locations to measure the thickness of PDC deposits based on outcrops (blue circle), borehole (green circle), and topography (yellow circle) sites. The outcrop located at 166 km from the source is shown. The tephra fall outcrop locations at Omachi City, Nagano Prefecture, Noshiro City, Akita Prefecture, and Abashiri City, Hokkaido, are shown in the inset map (upper left corner).

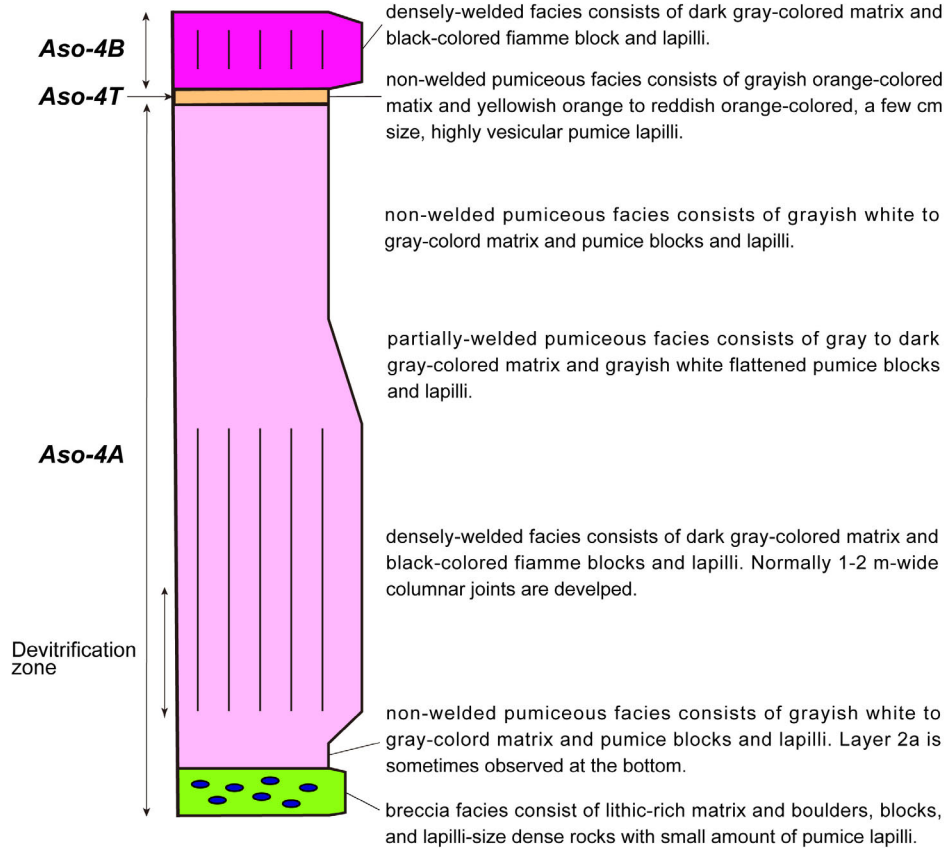

FIGURE 2 | Schematic columnar section of Aso-4 PDC deposit at the north and eastern side of Aso caldera area.

most voluminous of the Aso-4 units. The Aso-4T PDC deposits are relatively thin and distributed locally compared with the Aso-4A PDC deposits (**Figure 2**). The Aso-4T deposits are non-welded and consist of orange-gray matrix and yellowish-orange to reddish-orange-colored highly vesicular pumice lapilli. The size of the pumice clasts is usually less than a few cm. A relatively small amount of <1 cm-size lithic clasts are contained. The Aso-4T unit traveled as far as 166 km from the source. The upper Aso-4B deposits are densely welded and consist of dark-gray matrix and black-colored fiamme block and lapilli (**Figure 2**). The thickness of the Aso-4 PDC deposits decreases in the distal facies (**Figure 3e**). The densely welded ca. 100–400 m-thick intra-caldera Aso-4 PDC deposits are found from the borehole samples at −800 to −1000 m a.s.l. within the steep-sided low-gravity zone (Hoshizumi et al., 1997; Komazawa, 1995; NEDO, 1995).The measured densities of Aso-4 PDC welded facies are 1,690, and 1,810 (partially welded), 2,240, 2,260, and 2,270 (densely welded) kg/m^3 (mean is about 2,000 kg/m^3) and the non-welded facies is about 1,100 kg/m^3. Published values for the measured densities of Aso-4 PDC welded facies range from 1,500–2,450 kg/m^3 (mean is about 2000 kg/m^3; Suzuki and Ono, 1963; Suzuki, 1970; Urai and Tsu, 1986; Yamaguchi et al., 2000) and the non-welded facies is about 1,100 kg/m^3 (e.g., Suzuki, 1970). The degree of welding of Aso-4 PDC deposits ranges between welded rank II (1,250–1,650 kg/m^3) and VI (>2,300 kg/m^3), according to the classification of Quane and Russell (2005).

Petrological studies of Aso-4 PDC deposits were made by Lipman (1967), Watanabe (1978, 1979), Hunter (1998), Kaneko et al. (2007), Miyoshi et al. (2011), and Ushioda et al. (2020). Watanabe (1978, 1979) and Kaneko et al. (2007) showed that the magma of the Aso-4 PDC deposits were derived from homogeneous, voluminous felsic magma sources (SiO_2 = 66–70%) and heterogeneous, low volume mafic magmas (SiO_2 = 50–57%). Kaneko et al. (2007) discussed that the Aso-4 PDC deposits are characterized by two cycles of initial voluminous felsic magmas followed by mafic and mixed magmas.

Matsumoto et al. (1991) and Matsumoto (1996) defined a K-Ar age of 89 ± 7 ka for the Aso-4 deposit. Yoshikawa and Kuwae (2001), Nagahashi et al. (2004, 2007), and Tsuji et al. (2018) similarly defined age of 87 ka (Marine Isotope Stage, MIS5.2) based on tephra correlations with marine tephras. Therefore, the eruption age of the Aso-4 event is considered to be 87–89 ka.

Machida et al. (1985) and Machida and Arai (2003) estimated the volume of Aso-4 PDC deposit at >200 km^3 and Aso-4 tephra fall at >400 km^3. Suto et al. (2007) estimated the total volume of the tephra fall deposit at 1,051 km^3. Yamamoto (2015) estimated the total volume at 384 km^3 in DRE (dense rock equivalent;

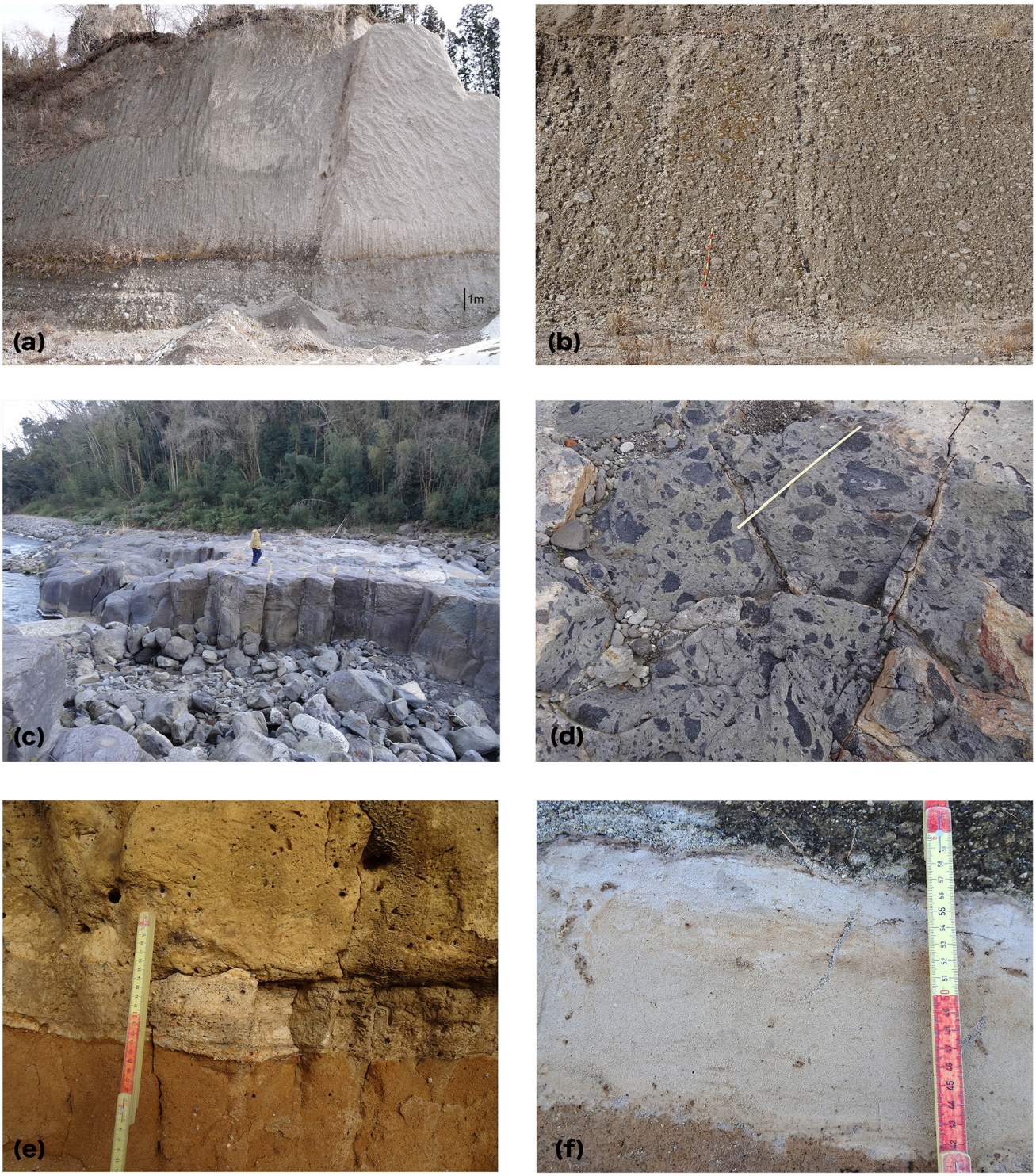

FIGURE 3 | Typical outcrops of Aso-4 PDC and tephra fall deposits. **(a)** Non-welded facies (11 km SE from the source). The lower part is the breccia facies. **(b)** Enlargement of the non-welded facies (30 km N). The scale is 1 m long. **(c)** Welded facies (33 km ENE). **(d)** Enlargement of the welded facies. Note plan view of fiammes [location is the same as **(c)**]. **(e)** Distal facies of the 10–15 cm-thick Aso-4 PDC deposit (white and pale orange-colored part, 117 km NNW). **(f)** A 12 cm-thick Aso-4 tephra fall deposit at Shari Town, Hokkaido (1,695 km NE from the source).

Walker, 1980). Nakajima and Maeno (2015) estimated the total volume at 200 km^3 in DRE.

METHODS AND RESULTS

Distribution and Thickness Estimation of Aso-4 PDC Deposits

The distribution of the current exposure of Aso-4 PDC deposits (**Figures 1**, **4**) was compiled based on geological maps, such as 1:50,000 and 1:200,000 Geological Maps published by Geological Survey of Japan (GSJ), 1:50,000 Surface Geological Maps published by Ministry of Land, Infrastructure and Tourism (MLIT), and maps in published papers. The distribution of the current exposure of Aso-4 PDC deposits was traced using GIS software. The Aso-4 PDC distributions are not shown in areas that have been covered subsequently by thick tephra fall deposits (e.g., the eastern part of Aso caldera) and the younger Kuju volcanic area (30 km NE of Aso caldera).

The original distribution of Aso-4 PDC deposits just after the eruption was estimated by integrating observations and data from current distributions, topographic maps, published papers, and boreholes (**Figures 4–7**). The distal runout distribution limit of Aso-4 PDC deposits in the sea area is assumed to be oval in shape (Machida et al., 1985; Machida and Arai, 2003), as shown in **Figure 5**. The maximum runout distances and apparent friction coefficient (H/L ratio) of Aso-4 PDC deposits are different from the directions, according to the topography of the source region and their pass. For example, the maximum distances of the Aso-4 PDC deposits from the source depend on direction: 166 km (NNE direction), 123 km (WNW), 84 km (SSW), 97 km (SSE), and 80 km (E). Especially, SE to SW side of the Aso caldera is high mountain areas, where the Aso-4 PDC deposits were accumulated within the basins and valleys. Therefore, we think that the oval shape is more reasonable than circular. The Aso-4 PDC deposits were considered to fill the low-land area and valleys. The Aso-4 PDC deposits were assumed to be transferred by turbidity currents and traveled further along the submarine bottom surface topography. However, we considered the Aso-4 PDC that we infer traveled on the surface of the sea, ignoring the submarine processes after entering into submarine seawater. The thin ignimbrite veneer deposits (Walker, 1981) were locally

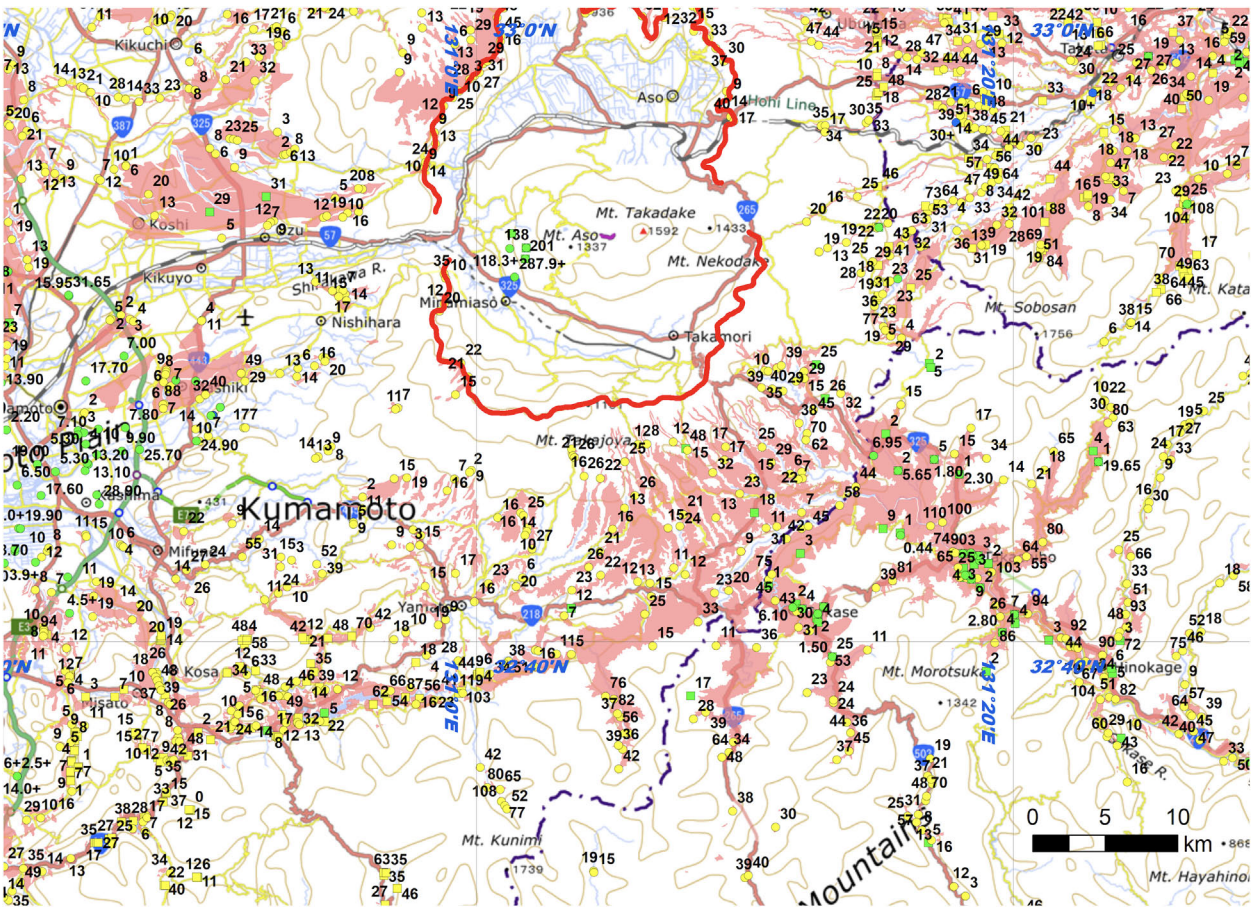

FIGURE 4 | Distribution of Aso-4 PDC deposits and thickness data. The thickness values of the deposits are shown in meters. Circles and squares on the map indicate locations to measure the thickness of PDC deposits based on outcrops (blue), borehole (green), and topography (yellow) sites. The circle marks are non-welded, and the square marks are welded points. The Geospatial Information Authority of Japan (GSI) Tile Map (English) is used as the base map.

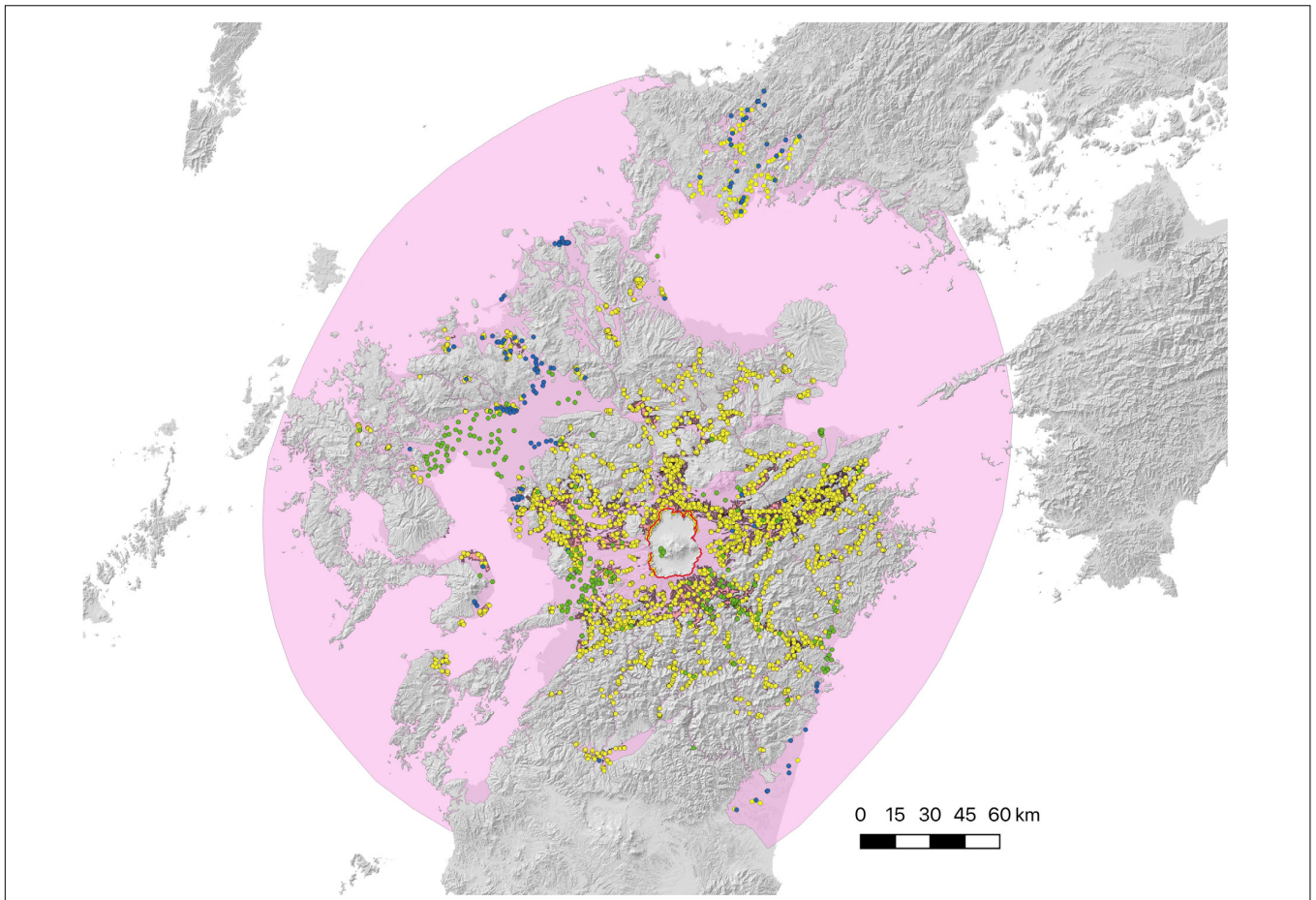

FIGURE 5 | Estimated original distribution of Aso-4 PDC deposit after the emplacement. Legends of circles on the map are the same as in **Figures 1**, **4**. The Geospatial Information Authority of Japan (GSI) Tile Map (Shaded relief map) is used as the base map.

preserved, but not considered on this map because the accurate mapping of such volumetrically minor material was not possible.

The thickness of the Aso-4 PDC deposits was measured using 1:200,000 Geological Maps and 1:50,000 Geological Maps published by GSJ, 1:50,000 Surface Geological Maps published by MLIT, borehole data KuniJiban Database provided by MLIT (MLIT, 2020) and Geo Station Database provided by the National Research Institute for Earth Science and Disaster Prevention (NIED) (NIED, 2020). Location, altitude, and depth of the top and bottom of the deposits in subsurface boreholes and welded (1,070 points) and non-welded (2,541 points) data were compiled (3,611 points in total; **Figures 1**, **4**–**7**). Partially welded facies are classified as non-welded in our compilation. Thickness data at outcrops obtained from published papers were used (blue circles in **Figures 1**, **4**, **5**, **7**). Thickness data were measured from the top and bottom depth of the Aso-4 deposits on the KuniJiban and Geo Station Databases (green circles in **Figures 1**, **4**–**7**; accuracy is about 10 cm). The thickness data were also measured from upper-limit and lower-limit altitudes on geological maps at ignimbrite plateau and measurable points (yellow circles in **Figures 1**, **4**–**7**). The thickness of the deposits within the caldera (118–407 m) was also measured using borehole data (Hoshizumi et al., 1997; Komazawa, 1995; NEDO, 1995). The thickness data were compiled in an excel spreadsheet and plotted using QGIS software.

Volume Estimation of Aso-4 PDC Deposits

The thickness data were analyzed within a 7 km × 5.5 km mesh grid (**Supplementary Table S1**). The maximum (**Figure 6a**), minimum (**Figure 6b**), and average (mean; **Figure 6c**) of each grid cell was calculated and plotted (purple-colored numbers values in **Figure 6**). For example, the 3rd cell from the right in the middle of **Figure 6** contains 6 thickness data of non-welded facies (48.9, 55.2, 34, 37, 9, and 50 m). Hence, the maximum, minimum, and average (mean) thickness are 55.2 m, 9 m, and ca. 39 m, respectively. The thickness was plotted for non-welded facies (**Figures 6**, **7b**) and also welded facies (**Figure 7a**). The grid cells that contain no thickness data were estimated using the ordinary kriging method (geospatial interpolation; Davis, 1986; Yamamoto, 2000). When the thickness value became <0 m, the estimated thickness was assigned to be 0 m. In the sea area, the marginal thickness was set at 0 m (right-lower corner of

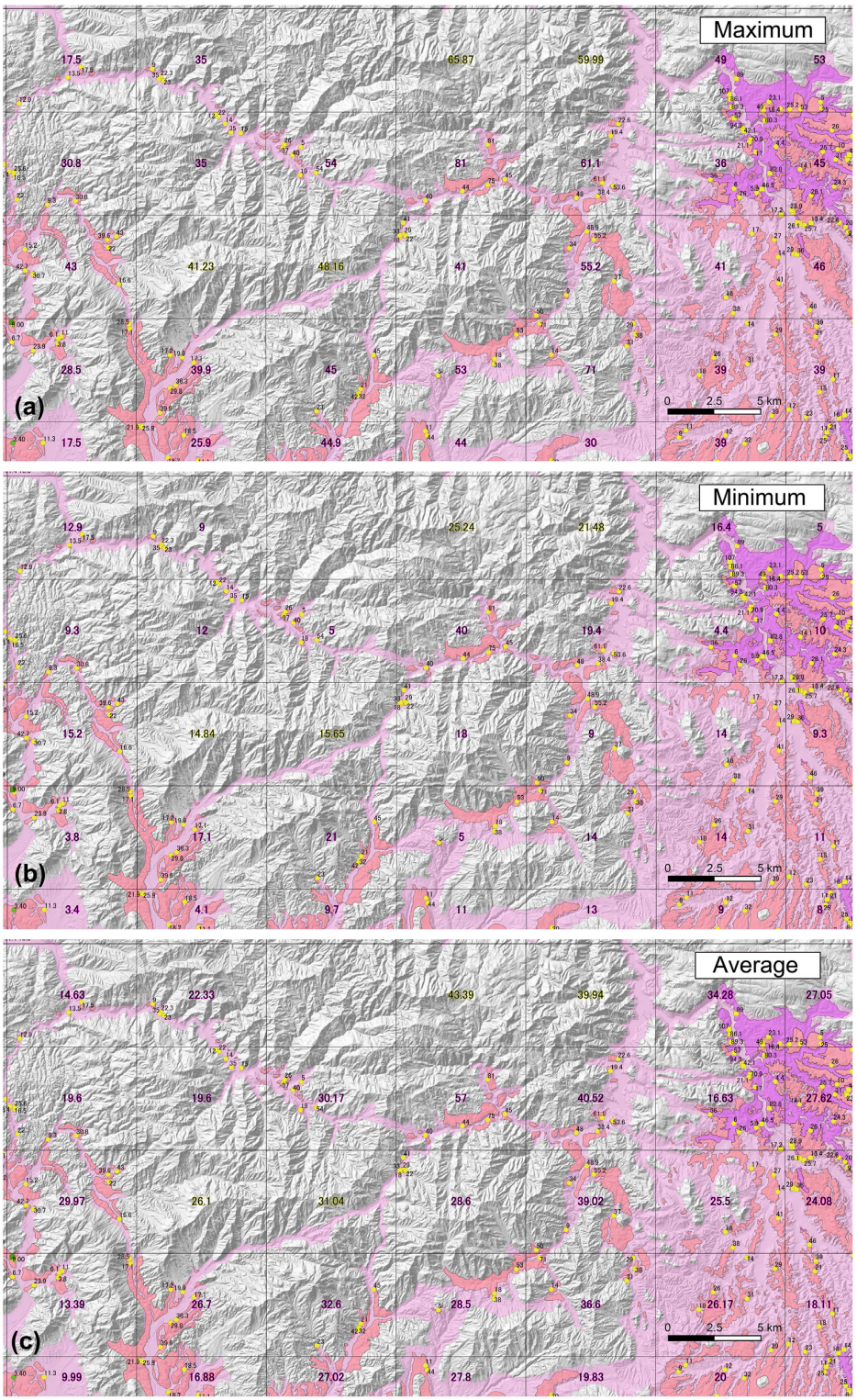

FIGURE 6 | Estimated thickness of non-welded parts of Aso-4 PDC deposits [maximum **(a)**, minimum **(b)**, and average (mean) cases **(c)**] at NW side of Aso caldera. Orange-colored parts are the non-welded facies of Aso-4 PDC deposits (current exposure). Purple-colored parts are the welded-facies (current exposure). Light pink-colored parts are the estimated original distribution of the Aso-4 PDC deposit. Purple-colored rim numbers are the maximum **(a)**, minimum **(b)**, and average **(c)** thickness values (m) of all points data within the cell. Yellow-colored rim numbers are the estimated thickness values using the ordinary kriging method. Circles and Squares on the map indicate locations to measure the thickness of PDC deposits based on borehole (green) and topography (yellow) sites. The circle marks are non-welded, and the square marks are welded points. The Geospatial Information Authority of Japan (GSI) Tile Map (Shaded relief map) is used as the base map.

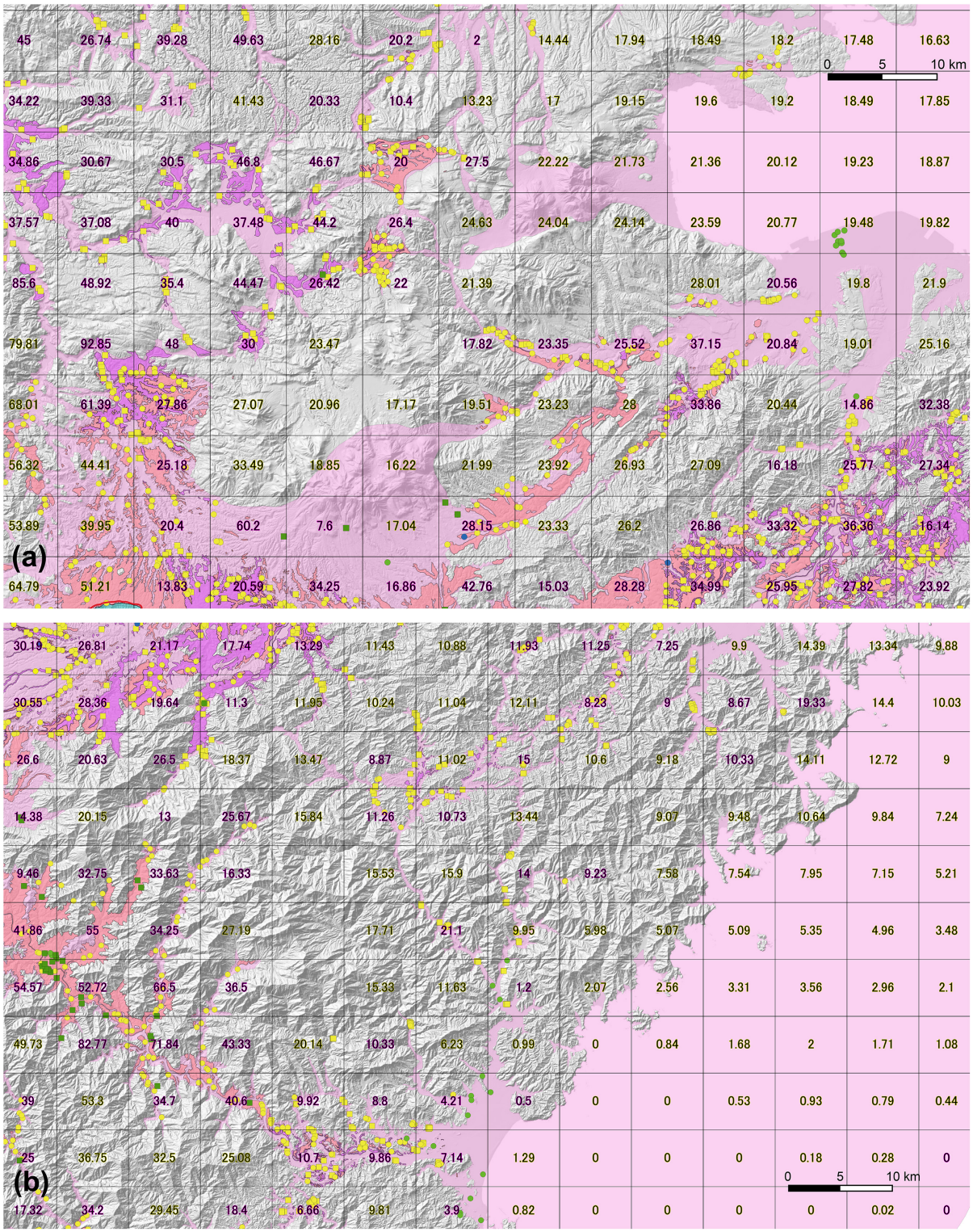

FIGURE 7 | Estimated thickness of Aso-4 PDC deposit. Welded PDC deposits at N and NE side of Aso caldera **(a)** and non-welded PDC deposits at E and SE side of Aso caldera **(b)**. Orange-colored parts are the non-welded facies of Aso-4 PDC deposits (current exposure). Purple-colored parts are the welded-facies (current exposure). Light pink-colored parts are the estimated original distribution of the Aso-4 PDC deposit. Purple-colored rim numbers are the average (mean) thickness of all points data within the cell. Yellow-colored rim numbers are the estimated thickness values using the ordinary kriging method. Symbol colors and type of point data are the same as **Figure 6**. The Geospatial Information Authority of Japan (GSI) Tile Map (Shaded relief map) is used as the base map.

TABLE 1 | Results of the area and volume estimation of Aso-4 PDC deposit (density of the non-welded and unclassified facies is 1,100 kg/m^3, welded facies is 2,000 kg/m^3, and dense rock is 2,500 kg/m^3).

		Area (km^2)	Volume (km^3 Bulk)			Volume (km^3 DRE)		
			Maximum	Minimum	Average	Maximum	Minimum	Average
Current Exposure	Non-welded and unclassified	1,007	37.1	7.6	21.3	16.3	3.4	9.4
	Welded	336	16.6	5.6	10.9	13.3	4.5	8.7
	Subtotal	1,343	53.7	13.2	32.1	29.6	7.8	18.0
Original Distribution (outflow)	Non-welded and unclassified	–	288.9	82.8	173.8	127.1	36.4	76.5
	Welded	–	429.3	163.5	296.7	343.4	130.8	237.4
	Subtotal	34,324	**718.2**	**246.2**	**470.5**	**470.6**	**167.2**	**313.8**
Intracaldera	Non-welded and unclassified	–	145.4	42.3	105.8	64.0	18.6	46.5
	Welded	–	71.9	49.3	64.3	57.6	39.5	51.4
	Subtotal	357	217.4	91.6	170.1	121.5	58.1	98.0
	Total	34,681	**935.6**	**337.9**	**640.5**	**592.1**	**225.3**	**411.8**

The bold numbers values are the most important values (results of our estimation).

Figure 7b), and the thickness of the PDC deposits (above the sea surface) was calculated using the ordinary kriging method. The thickness tends to decrease radially from the source toward the marginal rim in the sea area. The thickness of the deposits in the subaerial area changes according to the local topography. Local thickening of the PDC deposits is observed at the slope change or basin areas (such as the upper right of **Figure 6**, middle left and lower right of **Figure 7a**, and middle left of **Figure 7b**).

The occupied area of the estimated original Aso-4 PDC deposit (i.e., just after the deposition; the light-pink colored area in **Figures 6**, **7**) within each 7 km × 5.5 km grid cell was calculated using QGIS software. The maximum, minimum, and average volumes of each grid cell were calculated by multiplying the estimated thickness and area of the Aso-4 PDC deposit (volumes of non-welded and welded facies were calculated, separately). The total estimated bulk volume (km^3) was calculated by summing up all estimated volumes of grid cells. The DRE volume (**Table 1**) was calculated from the ratio between the average non-welded density (1,100 kg/m^3) and dense rock density (2,500 kg/m^3) and also the ratio between the average welded density (2,000 kg/m^3) and dense rock density (2,500 kg/m^3).

The results of the area and volume estimations of Aso-4 PDC deposits are summarized in **Table 1**. The current exposure area of the Aso-4 PDC deposit is about 1,000 km^2. The estimated original distribution area of the outflow Aso-4 PDC deposit (just after deposition) is about 34,000 km^2. Total volumes of the current exposure of Aso-4 PDC deposits are 13–54 km^3 in bulk (8–30 km^3 in DRE). The estimated original volumes of Aso-4 PDC outflow deposits are 250–720 km^3 (170–470 km^3 in DRE). The estimated original volumes of intracaldera Aso-4 PDC deposits are 90–220 km^3 (58–120 in DRE). The total estimated original volumes of Aso-4 PDC deposit just after deposition are 335–940 km^3 (225–590 km^3 in DRE; 5.6–14.8 × 10^{14} kg) (**Table 1**).

Distribution Estimation of Aso-4 Tephra Fall Deposits

Thickness and location data of Aso-4 tephra fall deposits are recompiled from prior studies, which comprise data for 71 locations of outcrops, lacustrine, submarine, and on-land cores and boreholes (**Supplementary Table S2**). The thickness data were plotted using ArcGIS software, and isopach maps (1, 2, 4, 8, 16, 32, 64, and 128 cm) of Aso-4 tephra deposits were made (**Figure 8**). The thickness of the tephra fall deposit in Eastern Hokkaido is up to 15 cm (**Figure 3f**). This value is relatively high compared to the Honshu area (probably due to local wind effects). Hence, two types of isopach maps were made: (1) Maximum case (**Figure 8a**), using the thickness data of Eastern Hokkaido and assuming erosion in the Honshu area; and (2) Minimum case (**Figure 8b**), for which the thickness data of Eastern Hokkaido were considered to be influenced by local wind disturbance and ignored for drawing.

Volume Estimation of Aso-4 Tephra Fall Deposits

The area of each isopach contour was calculated using ArcGIS software, and the volumes of Aso-4 tephra fall deposits were estimated using the segment integration method (Takarada et al., 2001, 2016). In the maximum case, the volume was calculated by integrating 3 subdivisions (**Figure 8a**; subdivided at 16 and 64 cm isopachs). In each segment, the data were plotted approximately on a straight line using the least square method. The volume was calculated for the area between the caldera rim (5.3 × 10^2 km^2) and the distal limit, for a total area of 10^8 km^2 (0.1 mm in thickness). The thickness of the tephra fall deposit at the caldera rim was assumed at 300 cm from the extrapolation of the trend of 64 and 128 cm isopach data. The average density of the tephra fall deposit was estimated at about 1,000 kg/m^3. The estimated results were 400 km^3 (4.0 × 10^{14} kg) in the area of the distal region (<16 cm isopach data area), 470 km^3 (4.7 × 10^{14} kg) in the medial region (between 16 and 64 cm data area), and 47 km^3 (4.7 × 10^{13} kg) in the area of the proximal region (between 64 and 300 cm data area). The total estimated eruptive mass of the Aso-4 tephra deposit was 920 km^3 (370 km^3 in DRE; 9.2 × 10^{14} kg).

In the minimum case, the volume was calculated by integrating three subdivisions (**Figure 8b**; subdivided at 4 and 64 cm isopach). The volume was also calculated for the area

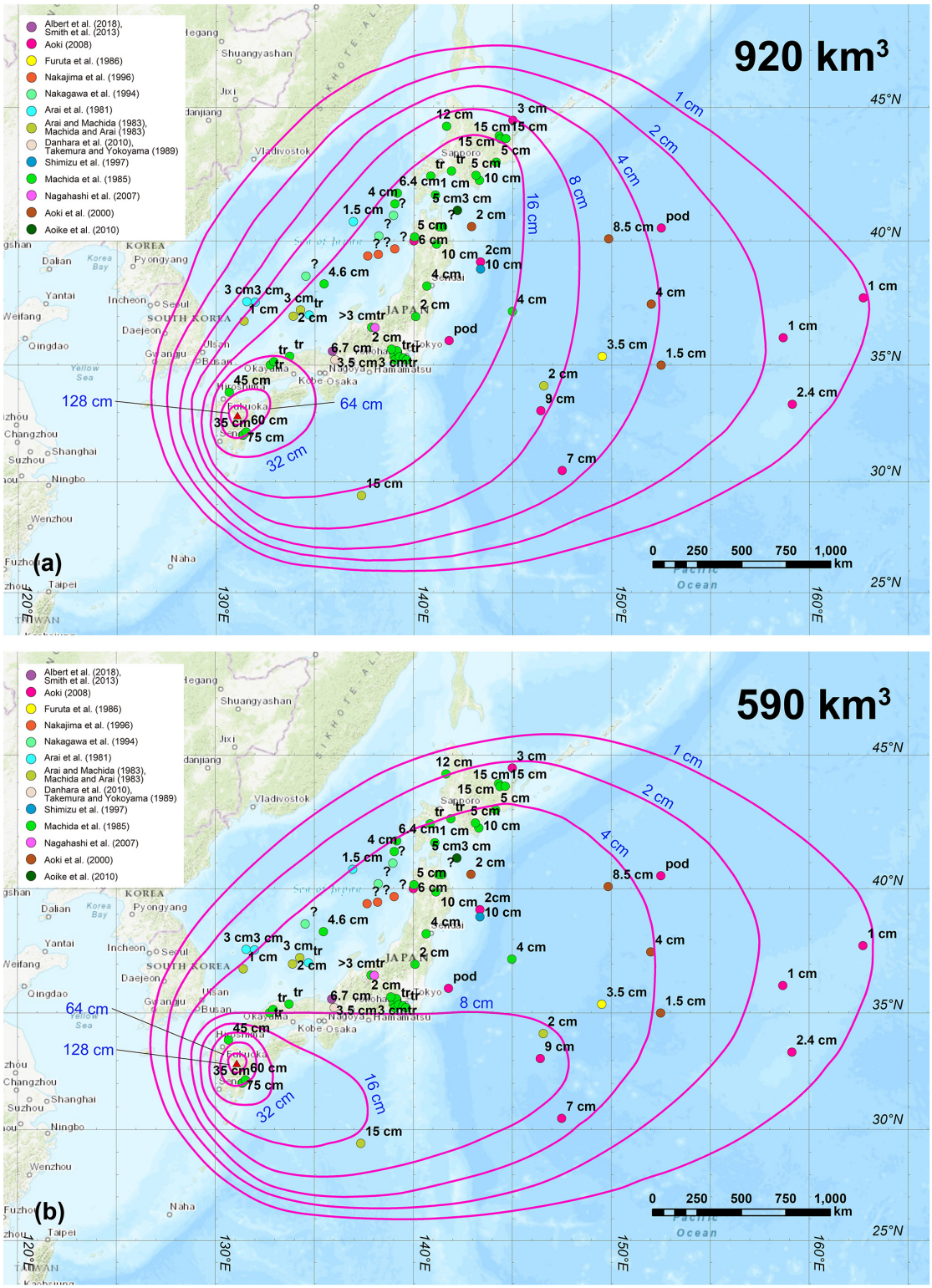

FIGURE 8 | Isopach maps of Aso-4 tephra fall distributions. Maximum case **(a)** and minimum case **(b)**. The data are tephra fall deposit from a borehole at Lake Suigetsu (Albert et al., 2018; Smith et al., 2013) (purple-colored circle), tephra fall deposit from a borehole at Lake Biwa (Takemura and Yokoyama, 1989; Danhara et al., 2010) (pale orange), submarine tephra deposits from Aoki (2008) (pink), Furuta et al. (1986) (yellow), Nakagawa et al. (1994) (light green), Nakajima et al. (1996) (orange), Arai et al. (1981) (light blue), Arai and Machida (1983) and Machida and Arai (1983) (greenish brown), Shimizu et al. (1997) (blue), Machida et al. (1985) (green), Aoki et al. (2000) (brown), and Aoike et al. (2010) (dark green), and on land tephra fall deposits from Machida et al. (1985) (green) and Nagahashi et al. (2007) (red purple).

between the caldera rim (5.3×10^2 km^2) and the distal limit, for a total area of 10^8 km^2. The thickness of the tephra fall deposit at the caldera rim was assumed at 300 cm. The estimated results were 170 km^3 (1.7×10^{14} kg) in the area of the distal region (<4 cm isopach data area), 380 km^3 (3.8×10^{14} kg) in the medial region (between 4 and 64 cm data area), and 45 km^3 (4.5×10^{13} kg) in the area of the proximal region (between 64 and 300 cm data area). The total estimated eruptive mass of the Aso-4 tephra deposit was 590 km^3 (240 km^3 in DRE; 5.9×10^{14} kg).

DISCUSSION

Aso-4 PDC Deposit Distributions and Volume

The original distributions of Aso-4 PDC deposits just after the emplacement were made based on the current distribution of the deposits, borehole data, and topographic data (**Figures 5–7**). This original estimated distribution is one of the most detailed maps of the Aso-4 PDC deposit, which shows the affected areas in this region. The current exposure area of the Aso-4 PDC deposit is about 1,000 km^2 (**Table 1**). The estimated original distribution area of the outflow Aso-4 PDC deposit (just after the emplacement) is about 34,000 km^2. Therefore, the area of estimated distribution is 34 times larger than the current deposit exposure. Most of the deposits were considered to be eroded, as observed for PDC deposits after the eruption of Pinatubo in 1991 (e.g., Major et al., 1996). This new map provides essential information for considering the affected area of the Aso-4 PDC and evaluating potential future eruption scenarios at Aso caldera. We assumed an oval shape for the distal limit of the Aso-4 PDC deposit, as shown in Machida et al. (1985) and Machida and Arai (2003). The estimation of the distal limit of the large-scale PDC is relatively difficult, especially in the sea area. Numerical simulations, such as the energy cone model (Malin and Sheridan, 1982), are one of the solutions.

Maximum, minimum, and average thickness data within each 7 km × 5.5 km mesh grid were calculated based on 3,611 thickness point data (**Figures 6**, **7**). The total estimated eruptive volume of the Aso-4 PDC deposits is 940 km^3 (590 km^3 DRE in maximum), 335 km^3 (225 km^3 DRE in minimum), and 640 km^3 (410 km^3 DRE in average) (**Table 1**). This result is about 1.7–4.7 times larger than the minimum value of the previous estimation at >200 km^3 (Machida and Arai, 2003). The main reason for the larger revised value is that this study was based on a much more detailed estimation of distributions and thicknesses data, including data not exposed on the surface (borehole data). This estimation method used a 7 km × 5.5 km mesh grid, making it one of the most detailed volume estimations of large-scale PDC deposits. This method can be used to accurately estimate the volumes of other caldera-forming large-scale PDC deposits around the world.

Volume estimation method uncertainties are herein considered. Factors that may have increased the upper limit bound are as follows. (1) The upper part of Aso-4 PDC deposits are sometimes eroded due to weathering since 87–89 ka, and thus the measured thickness data from the geological maps may be underestimated. (2) The unclassified point data are included in the non-welded facies. Some of them are considered to be welded facies (increase the DRE volume and eruptive mass). (3) The distribution of the ignimbrite veneer facies in the mountain area is not included in this estimation. The distance from the source to the coast area is about 70 km on average. Therefore, the area to the coast is ca. 1.5×10^4 km^2. The average thickness of the ignimbrite veneer facies is about 2 m (Watanabe, 1986; Suzuki-Kamata and Kamata, 1990). The total estimated volume of the veneer facies is estimated at about 30 km^3. This volume is about 3.2–9 % of the estimated total volume (335–940 km^3) of the Aso-4 PDC deposit.

Factors that may have decreased the lower limit bound are as follows. (1) The distribution limit in the sea area is considered as oval in shape; however, the original runout distance of the Aso-4 PDC deposits may be shorter locally due to the topographical barriers in the subaerial region. (2) The average density of the Aso-4 PDC deposits is decreasing according to the runout distance. The effect of the lower density of the distal facies tends to decrease the total DRE volume.

Another possible factor in changing the upper and lower bounds is the fact that the ordinary kriging method is used for the estimation of no-measured thickness data area by the extrapolation of the surrounding measured area data. This estimation does not integrate the PDC dynamics (e.g., local deposition due to topographic changes such as slope and valley width changes). The thickness may change if the PDC dynamics are included. Future studies such as numerical simulations, including deposition processes from the bottom of the PDC, are needed.

Aso-4 Tephra Fall Distributions and Volume

The estimated volumes of Aso-4 tephra fall (590–920 km^3; 240–370 km^3 in DRE) became larger than the minimum value of the previous estimation (>400 km^3; Machida et al., 1985; Machida and Arai, 2003). The estimation result is about 56–88% volume of the estimation (1,051 km^3) by Suto et al. (2007). The main reasons for the calculation of a larger volume compared to the Machida et al. (1985) and Machida and Arai (2003) in this study are: (1) the isopach map area became much larger than the previous estimation due to the inclusion of more submarine tephra fall data; and (2) the calculation method is different from the previous estimation. Machida et al. (1985) and Machida and Arai (2003) estimated the eruptive volume of the Aso-4 tephra fall using the extended area (>4×10^6 km^2) multiplied by the average thickness of 10 cm. Suto et al. (2007) estimated the eruptive volume of the Aso-4 tephra fall deposits using GIS software and the isopach map published by Machida et al. (1985) and Machida and Arai (2003). However, no details of the calculation methodology were provided in the paper. The purpose of their paper was to make a tephra fall database covering the whole of Japan. The results of such volume estimations are preliminary and tend to have significant errors (e.g., Yamamoto, 2017).

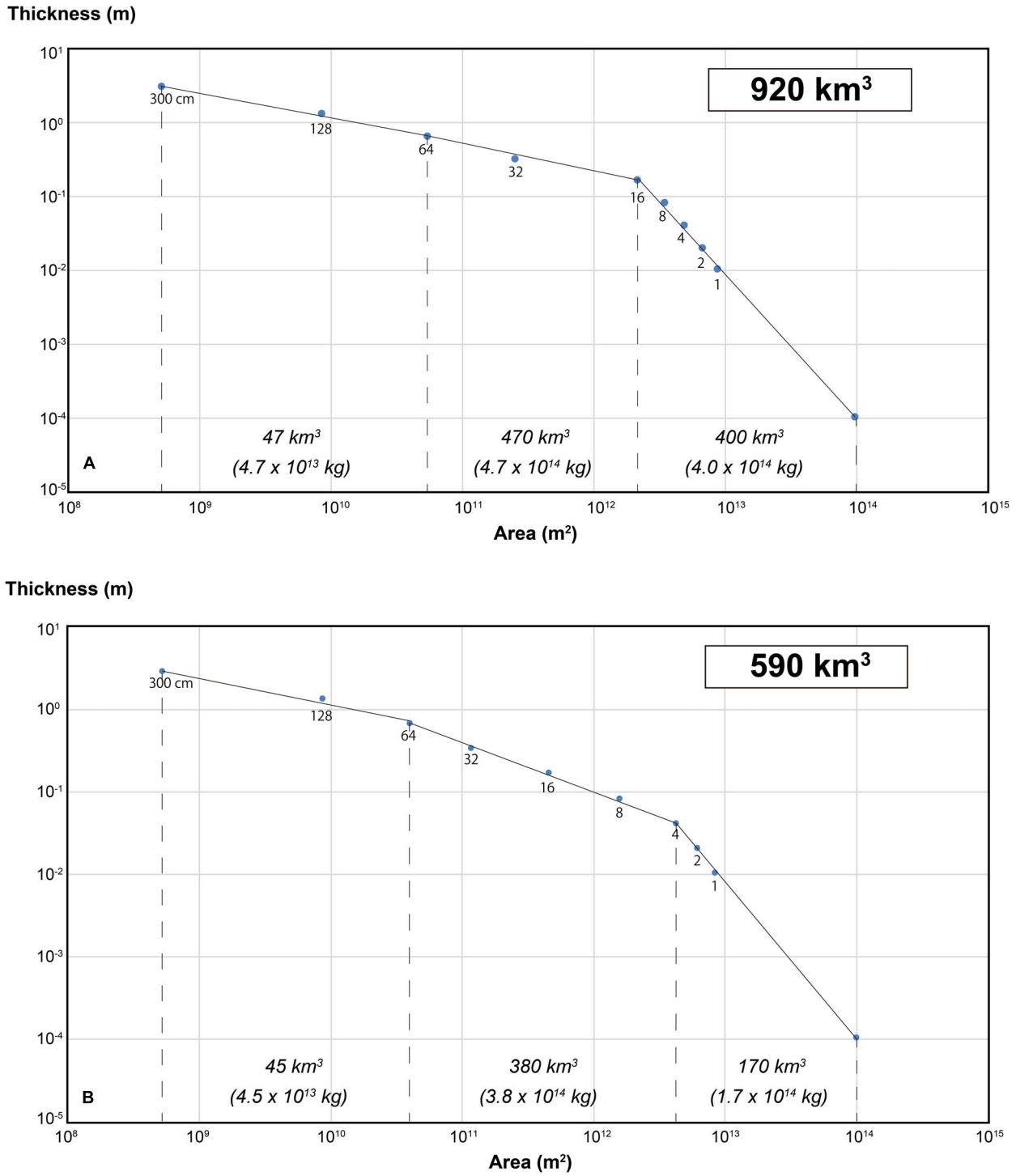

FIGURE 9 | Estimation results of Aso-4 tephra fall deposits using the segment integration method. Maximum case **(A)** and minimum case **(B)**.

Uncertainties in tephra fall volume estimates originate with several factors. Factors that may have increased the upper limit bound are as follows. (1) Especially relatively thin tephra fall deposits in the distal regions are quickly eroded by wind and rainfall. The tephra deposits are preserved only in limited areas such as lakes, swamps, and peatlands. Even if the tephra was deposited in these areas, the original thickness might not be preserved (the original deposit thickness may be thicker than the current thickness). (2) The submarine tephra fall deposits are possibly diffused due to the submarine currents while settling on

the bottom of the sea (other factors than the wind diffusion). (3) In this tephra fall volume estimation, up to 10^8 km^2 areas are calculated (**Figure 9**). Although, cryptotephras derived from the co-ignimbrite tephra falls are possibly distributed more widely as the Earth's surface area, especially for such a large-scale eruption case (e.g., Abbott and Davies, 2012; Davies, 2015). When the cryptotephra distributed to the area as large as on the Earth's surface (5.1×10^8 km^2; five times larger than the current extent), the estimated total tephra volume is 930 km^3 in maximum (extrapolated the decreasing trend of 16 cm to 1 cm isopach maps; **Figure 9A**). The difference is 10 km^3, indicating that the effect of the far distal area is about 1% of the total tephra volume.

The volume ratio of tephra fall deposits in the proximal area (64–300 cm thickness segment) is relatively small compared to the total eruptive volume (45–47 km^3; 5–7%; **Figure 9**). Even if the calculation area is extended up to a vent size (e.g., 0.01 km^2), the result of the total volume is not changed (590–920 km^3). The volume ratio in the proximal area against the total volume is different from other types of eruption. For example, the volume ratio of tephra fall deposits in the proximal area (between 0.45 and 1.5 kg/m^2) against the total volume of the 2014 Ontake phreatic eruption is 38% (4.5×10^8 kg/1.18×10^9 kg) (Takarada et al., 2016). These differences are probably due to the different eruption mechanisms between the two types of tephra falls (large-scale Plinian and small-scale phreatic eruptions).

Factors that may have decreased the lower limit bound are as follows. (1) The Aso-4 PDC deposits are subdivided into eruptive units with cooling unit hiatuses (e.g., Watanabe, 1978), suggesting the duration of the Aso-4 eruption lasted for more than a few days to months. The isopach map may consist of a combination of several isopach maps with the different wind directions. In this case, the total tephra fall volume may be decreased due to a combination of narrow isopach maps. (2) For the tephra fall deposits in the lacustrine and submarine areas, it is possible that the thickness of the deposit is sometimes increased due to reworking by bottom currents in such settings.

Another possible factor to consider in changing the upper and lower bounds is that we used the segment integration method, which enables relatively accurate mathematical calculations (Takarada et al., 2001, 2016). Other tephra fall estimation methods such as Exponential fit (Pyle, 1989), Power-law fit (Bonadonna and Houghton, 2005), and Weibull fit (Bonadonna and Costa, 2012), however, are essential to check our estimation results. Such considerations will be addressed in a subsequent study.

Eruptive Volume of Aso-4 Eruption

The total eruptive volume of the Aso-4 eruption was estimated at 930–1,860 km^3 (465–962 km^3 in DRE; 1.2–2.4 $\times$ 10^{15} kg). This result is about 1.5–3.1 times larger than the minimum volume of the previous estimation by Machida and Arai (2003; >600 km^3), 1.1–2.3 times larger than [Yamamoto (2015); 384 km^3 in DRE], and 2.2–4.5 times larger than Nakajima and Maeno (2015; 200 km^3 in DRE). The reason for the larger revised volume is mainly due to more accurate estimations of distributions and thicknesses based on detailed datasets and different estimation methods. The eruption magnitude [$M = log_{10}$*(erupted mass (kg))-7*; Hayakawa, 1993; Pyle, 2000] is calculated at M8.1–8.4. The Aso-4 caldera-forming eruption is now considered to be one of the M8 (VEI8) class super-eruptions. This is the largest eruption in Japan in the last 100 ka. The eruptive volume of the 30 ka Aira eruption is estimated at 940–1,040 km^3 (380–430 km^3 in DRE; Takarada, 2019). The eruptive volume of the 106 ka Toya eruption is estimated at 230–310 km^3 (100–140 km^3 in DRE; Takarada, 2019; Tomiya and Miyagi, 2020). The Aso-4 eruption is about 0.8–2 times larger than the Aira eruption and about 3–8 times larger than the Toya eruption.

The eruptive volume of the 75 ka Youngest Toba Tuff derived from the Toba caldera is estimated at 13,200 km^3 (5,300 km^3 in DRE) (Costa et al., 2014). The eruptive volume of the 25.4 ka Oruanui eruption in the Taupo Volcanic Zone is estimated at 530 km^3 in DRE (Wilson, 2001; Vandergoes et al., 2013). Thus, the Aso-4 eruption is the 2nd largest eruption in the world in the last 100 ka. The eruptive volume of the 27.8 Ma Fish Canyon Tuff from the La Carita caldera, San Juan Volcanic Field, is estimated at 5,000 km^3 (Lipman et al., 1997; Bachmann et al., 2002). The eruptive volume of the 2.1 Ma Hukleberry Ridge Tuff derived from the Yellowstone caldera is estimated at 2,450 km^3 (Christiansen, 2001; Ellis et al., 2012). The eruptive volume of the 1.6 Ma Otowi Member of Bandelier Tuff derived from the Valles caldera is 216–550 km^3 in DRE (Cook et al., 2016). The Aso-4 eruption is one order smaller compared to the VEI 9 Youngest Toba Tuff (the largest volcanic eruption in the Quaternary), and 0.9–1.8 times larger than the Orunaui eruption in the Taupo Volcanic Zone. The Aso-4 eruption is 12–18% volume of the Fish Canyon Tuff (one of the largest ignimbrites in the world), 40–80% volume of the Hukleberry Ridge Tuff (the largest eruption from the Yellowstone), and slightly larger than the Otowi Member of Bandelier Tuff.

The total eruptive mass is estimated at 1.2–2.4 $\times$ 10^{15} kg. The Aso-4 PDC deposits consist of 8 eruptive units, which sometimes show discontinuities of welding degree and cooling unit hiatuses between them (e.g., Watanabe, 1978); thus, the volume of 1 flow unit (1 event) is on the order of 10^{13}–10^{14} kg. For example, if an event occurred within a period of 10–60 min, the average mass flow rate (MFR) is calculated at 10^9–10^{11} kg/s. The numerical 3D simulation suggests that the expected eruption column height of co-ignimbrite tephra fall would be as high as 40–60 km at this MFR (Costa et al., 2018). A significant global climate and environmental impact would occur from such a large eruption column due to the release of a large amount of volcanic gas (SO_2, HCl, and HF) (e.g., Rampino and Self, 1982; Trenberth and Dai, 2007; Kravitz and Robock, 2011). Long-term catastrophic effects on vegetation and ecosystem would be expected (e.g., Costa et al., 2014). Interaction with rainfall would cause the tephra fall deposits covering Japan to produce abundant lahars over large areas for more than 10 years (e.g., a large number of lahars occurred due to the ca. 10 km^3 1991 Pinatubo eruption for more than 10 years; Major et al., 1996). Therefore, a M8 class super-eruption would cause long-term severe volcanic hazards. Further studies on climate and volcanic hazard assessments are necessary.

The estimated distributions and eruptive volume of the Aso-4 PDC and tephra fall deposits are considered to become an essential dataset for volcanological, geophysical, and petrological

investigations, and volcanic hazard assessments for large-scale super-eruptions. This volume data is also useful to establish a more precise volume vs. time diagram of Aso volcano. The distribution and thickness data are useful for future studies on volcanic hazards. Research efforts on the estimation of the eruptive volume of other large-scale eruptions in Japan, such as Aira, Toya, Kutcharo, and Towada calderas, were made recently (e.g., Takarada et al., 2017, 2018; Takarada, 2019). Reevaluation of the eruptive volumes of major caldera-forming eruptions in other countries is also crucial. The estimation methods outlined in this contribution are applicable to any other large-scale caldera-forming eruptions and will enable the progression of similar volcanological research worldwide.

CONCLUSION

Detailed distributions of 87–89 ka Aso-4 PDC deposits were made based on published papers, geological maps, and borehole data (**Figures 5–7**). Thickness data were compiled from a total of 3,611 outcrops, geological maps, and borehole locations. The volume was calculated using thickness data and area of PDC deposit within each 7 km × 5.5 km mesh grid. The ordinary kriging method was used when no thickness data existed in the mesh grid. The maximum, minimum, and average volumes were calculated. The total eruptive volume of the Aso-4 PDC deposit was estimated at 340–940 km^3 (225–590 km^3 in DRE). The volume of co-ignimbrite Aso-4 tephra fall was estimated using two new isopach maps based on 71 submarine, lacustrine, and subaerial tephra deposits. The estimated volume of the Aso-4 tephra fall was 590–920 km^3 (240–370 km^3 in DRE), using the segment integration method (Takarada et al., 2001, 2016).

The total estimated eruptive volume of the Aso-4 eruption was 930–1,860 km^3 (465–960 km^3 in DRE; 1.2–2.4 × 10^{15} kg). Therefore, the Aso-4 eruption is now considered to have been a M8.1-8.4 (VEI 8) super-eruption. The Aso-4 eruption is the largest volcanic eruption in Japan and considered to be the 2nd largest eruption in the world in the last 100 ka. It is expected that these estimation results will provide essential parameters for long-term eruption forecasting, evaluation of volcanic activities, quantitative geophysical and petrological research work, and future volcanic hazards assessment. The proposed estimation method can be applied to any large-scale caldera-forming eruptions in the world for the reevaluation of eruptive volumes of PDC and tephra fall deposits.

DATA AVAILABILITY STATEMENT

The raw data supporting the conclusions of this article are available in the **Supplementary Material**. We include the data on location, area, measured thickness, estimated thickness (using ordinary kriging method), and original and current exposure volume in each mesh of the Aso-4 PDC deposits (**Supplementary Table S1**). Location, thickness, and references of the Aso-4 tephra fall deposits are also provided (**Supplementary Table S2**).

AUTHOR CONTRIBUTIONS

ST and HH conducted the fieldwork, compiled the data, determined the distribution of the Aso-4 PDC and tephra fall deposits, and undertook data interpretation as well as the refinement of this article.

FUNDING

This study was partly supported by the Secretariat of the Nuclear Regulation Authority, Japan.

ACKNOWLEDGMENTS

We acknowledge valuable discussions with Nobuo Geshi, Takashi Kudo, Teruki Oikawa, Isoji Miyagi, and Akihiko Tomiya of Geological Survey of Japan, AIST, and Yasuo Miyabuchi of Kumamoto University. We thank Sanko Consultant Co., Ltd., for all the support to compile the datasets. We also thank Christopher Conway and Joel Bandibas of Geological Survey of Japan, AIST, for checking the English of the manuscript. We are grateful for the detailed and valuable comments from two reviewers, AC and GV, and chief editor, Valerio Acocella, who allowed us to improve the manuscript.

SUPPLEMENTARY MATERIAL

The Supplementary Material for this article can be found online at: https://www.frontiersin.org/articles/10.3389/feart.2020.00170/full#supplementary-material

REFERENCES

Abbott, P. M., and Davies, S. M. (2012). Volcanism and the Greenland ice-cores: the tephra record. *Earth Sci. Rev.* 115, 173–191. doi: 10.1016/j.earscirev.2012.09.001

Albert, P. G., Smith, V. C., Suzuki, T., Tomlinson, E. L., Nakagawa, T., McLean, D., et al. (2018). Constraints on the frequency and dispersal of explosive eruptions at Sambe and Daisen volcanoes (South-West Japan Arc) from the distal Lake Suigetsu record (SG06 core). *Earth Sci. Rev.* 185, 1004–1028. doi: 10.1016/j.earscirev.2018.07.003

Aoike, K., Nishi, H., Sakamoto, T., Iijima, K., Tsuchiya, M., Taira, A., et al. (2010). Paleoceanographic history of offshore Shimokita Peninsula for the past 800,000 years based on primary analyses on cores recovered by D/V CHIKYU during the shakedown cruises. *KASEKI (Fossils)* 87, 65–81. doi: 10.14825/kaseki.87.0_65

Aoki, K. (2008). Revised age and distribution of ca. 87 ka Aso-4 tephra based on new evidence from the northwest Pacific Ocean. *Quat. Int.* 178, 100–118. doi: 10.1016/j.quaint.2007.02.005

Aoki, K., Yamamoto, H., and Yamauchi, M. (2000). Late quaternary tephrostaratigraphy of marine cores collected during "Mirai" MR98-03 and MR99-K04 cruises. *Report of Japan Marine Science and Technology Center* 41, 49–55. doi: 10.1016/j.envpol.2018.11.018

Arai, F., and Machida, H. (1983). "Deep submarine tephra catalogue around Japan Island," in *Research on Quaternary Volcanic Activities and Climate Change*

Mainly for the Deep Marine Deposits Analysis in and Around Japan. Report of Grant-in-Aid for Co-Operative Research (A) 56390016, ed. H. Machida (Tokyo: Japan Soc. Promotion of Science), 7–34.

Arai, F., Oba, T., Kitazato, H., Horibe, Y., and Machida, H. (1981). Late Quaternary tephrochronology and paleo-oceanography of the sediments of the Japan Sea. *Quat. Res.* 20, 209–230. doi: 10.4116/jaqua.20.209

Bachmann, O., Dungan, M. A., and Lipman, P. W. (2002). The fish canyon magma body, San Juan Volcanic Field, Colorado: rejuvenation and eruption of an upper-crustal Batholith. *J. Petrol.* 43, 1469–1503. doi: 10.1093/petrology/43.8.1469

Bonadonna, C., and Costa, A. (2012). Estimating the volume of tephra deposits: a new simple strategy. *Geology* 40, 415–418. doi: 10.1130/G32769.1

Bonadonna, C., and Houghton, B. F. (2005). Total grain-size distribution and volume of tephra-fall deposits. *Bull. Volcanol.* 67, 441–456. doi: 10.1007/s00445-004-0386-2

Christiansen, R. L. (2001). *The Quaternary and Pliocene Yellowstone Plateau Volcanic Field of Wyoming, Idaho, and Montana. U. S. Geological Survey Professional Paper 729-G*. Reston, VA: USGS. doi: 10.3133/pp729G

Cook, G. W., Wolff, J. A., and Self, S. (2016). Estimating the eruptive volume of a large pyroclastic body: the Otowi Member of the Bandelier Tuff, Valles caldera, New Mexico. *Bull. Volcanol.* 78:10. doi: 10.1007/s00445-016-1000-0

Costa, A., Smith, V. C., Macedonio, G., and Matthews, N. E. (2014). The magnitude and impact of the Youngest Toba Tuff super-eruption. *Front. Earth Sci* 2:16. doi: 10.3389/feart.2014.00016

Costa, A., Suzuki, Y. J., and Koyaguchi, T. (2018). Understanding the plume dynamics of explosive super-eruptions. *Nat. Commun.* 9:654. doi: 10.1038/s41467-018-02901-0

Danhara, T., Yamashita, T., Iwano, H., Takemura, K., and Hayashida, A. (2010). Chronology of the 1400-m core obtained from Lake Biwa in 1982-1983: Re-investigation of fission-track ages and tephra identification. *Quat. Res.* 49, 101–119. doi: 10.4116/jaqua.49.101

Davies, S. M. (2015). Cyrptotephras: the revolution in correlation and precision dating. *J. Quat. Sci.* 30, 114–130. doi: 10.1002/jqs.2766

Davis, J. C. (1986). *Statistic and Data Analysis in Geology -Second Edition*. Hoboken, NJ: Wiley.

Ellis, B. S., Branney, M. J., Barry, T. L., Barfod, D., Bindeman, I., Wolff, J. A., et al. (2012). Geochemical correlation of three large-volume ignimbrites from the Yellowstone hotspot track, Idaho, USA. *Bull. Volcanol.* 74, 261–277. doi: 10.1007/s00445-011-0510-z

Endo, H., and Suzuki, Y. (1986). *Geology of the Tsuma and Takanabe District. Quadrangle Series, 1:50,000*. Tsukuba: Geological Survey of Japan.

Engwell, S. L., Sparks, R. S. J., and Aspinall, W. P. (2013). Quantifying uncertainties in the measurement of tephra fall thickness. *J. Appli. Volcanol.* 2:5. doi: 10.1186/2191-5040-2-5

Fierstein, J., and Nathenson, M. (1992). Another look at the calculation of fallout tephra volumes. *Bull. Volcanol.* 54, 156–167. doi: 10.1007/BF00278005

Furuta, T., Fujioka, K., and Arai, F. (1986). Widespread submarine tephras around Japan-Petrographic and chemical properties. *Mar. Geol.* 72, 125–142. doi: 10.1016/0025-3227(86)90103-9

Hayakawa, Y. (1993). Proposal of eruption magnitude. *Bull. Volcanol. Soc. Japan* 6, 223–226. doi: 10.18940/kazan.38.6_223

Hayakawa, Y. (1995). One million-year chronology of volcanic eruptions in Japan using master tephras. *Bull. Volcanol. Soc. Japan* 40, S1–S15. doi: 10.18940/kazan.40.Special_S1

Henry, C. H. (2008). Ash-flow tuffs and paleovalleys in northeastern Nevada: implications for Eocene paleogeography and extension in the Sevier hinterland, northern great Basin. *Geosphere* 4, 1–35. doi: 10.1130/GES00122.1

Hoshizumi, H., Ono, K., Mimura, K., and Noda, T. (1988). *Geology of the Beppu District. Quadrangle Series, 1:50,000*. Tsukuba: Geological Survey of Japan.

Hoshizumi, H., Watanabe, K., Sakaguchi, K., Uto, K., Ono, K., and Nakamura, T. (1997). The Aso-4 pyroclastic flow deposit confirmed from the deep drill holes inside the Aso caldera. *Program. Abstracts Volcanol. Soc. Jpn* A05:5. doi: 10.18940/vsj.1997.2.0_5

Hunter, A. G. (1998). Intracrustal controls on the coexistence of tholeiitic and calc-alkaline magma series at Aso volcano, SW Japan. *J. Petrol.* 39, 1255–1284. doi: 10.1093/petroj/39.7.1255

Kamata, H. (1997). *Geology of the Miyanoharu District. Quadrangle Series, 1:50,000*. Tsukuba: Geological Survey of Japan.

Kandlbauer, J., and Sparks, R. S. J. (2014). New estimates of the 1815 Tambora eruption volume. *J. Volcanol. Geotherm. Res.* 286, 93–100. doi: 10.1016/j.jvolgeores.2014.08.020

Kaneko, K., Kamata, H., Koyaguchi, T., Yoshikawa, M., and Furukawa, K. (2007). Repeated large-scale eruptions from a single compositionally stratified magma chamber: an example from Aso volcano, Southwest Japan. *J. Volcanol. Geotherm. Res.* 167, 160–180. doi: 10.1016/j.jvolgeores.2007.05.002

Komazawa, M. (1995). Gravimetric analysis of Aso volcano and its interpretation. *J. Geodetic Soc. Jpn.* 41, 17–45. doi: 10.11366/sokuchi1954.41.17

Kravitz, B., and Robock, A. (2011). Climate effects of high-latitude volcanic eruptions: role of the time of year. *J. Geophys. Res.* 116:D01105. doi: 10.1029/2010JD014448

Legros, F. (2000). Minimum volume of a tephra fallout deposit estimated from a single isopach. *J. Volcanol. Geotherm. Res.* 96, 25–32. doi: 10.1016/S0377-0273(99)00135-3

Lipman, P. W. (1967). Mineral and chemical variations within an ash-flow sheet from Aso caldera, south-western Japan. *Cont. Mineral. Petrol.* 16, 300–327. doi: 10.1007/BF00371528

Lipman, P. W., Dungan, M., and Bachmann, O. (1997). Comagmatic granophyric granite in the Fish Canyon Tuff, Colorado: implications for magma-chamber processes during a large ash-flow eruption. *Geology* 25, 915–918. doi: 10.1130/0091-7613(1997)025<0915:CGGITF>2.3.CO;2

Machida, H., and Arai, F. (1983). Extensive ash falls in and around the Sea of Japan from large late Quaternary eruptions. *J. Volcanol. Geotherm. Res.* 18, 151–164. doi: 10.1016/0377-0273(83)90007-0

Machida, H., and Arai, F. (1988). A review of late quaternary deep-sea tephra around Japan. *Quat. Res.* 26, 227–242. doi: 10.4116/jaqua.26.3_227

Machida, H., and Arai, F. (2003). *Atlas of Tephra in and around Japan (Revised Edition)*. Tokyo: University of Tokyo Press.

Machida, H., Arai, F., and Momose, M. (1985). Aso-4 ash: a widespread tephra and its implications to the events of Late Pleistocene in and around Japan. *Bull. Volcanol. Soc. Japan* 30, 49–70. doi: 10.18940/kazanc.30.2_49

Major, J. J., Janda, R. J., and Daag, A. S. (1996). "Watershed disturbance and lahars on the east side of Mount Pinatubo during the mid-June 1991 eruptions," in *Fire and Mud Eruptions and Lahars of Mount Pinatubo, Philippines*, eds C. G. Newhall, and R. S. Punongbayan (Washington, DC: University of Washington Press), 895–919.

Malin, M. C., and Sheridan, M. F. (1982). Computer-assisted mapping of pyroclastic surges. *Science* 13, 637–640. doi: 10.1126/science.217.4560.637

Matsumoto, A. (1996). K-Ar age determinations of young volcanic rocks -correction for initial $^{40}Ar/^{36}Ar$ ratios and its application-. *Chishitsu News* 501, 12–17.

Matsumoto, A., Uto, K., Ono, K., and Watanabe, K. (1991). K-Ar age determination for Aso volcanic rocks -concordance with volcanostratigraphy and application to pyroclastic flows. *Program. Abstracts Volcanol. Soc. Jpn* 1991.2, B3, 73. doi: 10.18940/vsj.1991.2.0_73

Matsuo, S. (1978). The Pleistocene volcanic ash layers in Asahi Village and Ato Town, Abu County. *Nat. Yamaguchi Prefect.* 5, 12–18.

Matsuo, S. (1984). "An emissary from Kyushu," in *Yamaguchi Prefecture Geology Guide*, eds N. Murakami, Y. Nishimura, and Geological Soc. Yamaguchi (Tokyo: Corona Ltd.), 218–222.

Matsuo, S. (2001). Late Pleistocene-Holocene widely distributed volcanic ash in Yamaguchi Prefecture (no. 1) -Aso-4 pyroclastic flow deposit I. *Rep. Geol. Soc. Yamaguchi* 47, 1–12.

Matsuo, S., and Kawaguchi, T. (2015). Ube matsuyama cho volcanic Ash II and Aso pyroclastic flow unit "Aso-4 II". *Rep. Geol. Soc. Yamaguchi* 74, 8–14.

Matsuo, S., and Takahashi, Y. (1974). Discovery of Ube volcanic ash stratigraphy. *Rep. Geol. Soc. Yamaguchi* 7, 15–23.

Miyoshi, M., Shibata, T., Yoshikawa, M., Sano, T., Shinmura, T., and Hasenaka, T. (2011). Genetic relationship between post-caldera and caldera-forming magmas from Aso volcano, SW Japan: constraints from Sr isotope and trace element compositions. *J. Mineral. Petrol. Sci.* 106, 114–119. doi: 10.2465/jmps.101021b

MLIT (2020). *"KuniJiban" National Ground Information Database in Japan*. Tokyo: Ministry of Land, Infrastructure, Transport and Tourism.

Nagahashi, Y., Sato, T., Takeshita, Y., Tawara, T., and Kumon, F. (2007). Stratigraphy and chronology of widespread tephra beds intercalated in the

TKN-2004 Core sediment obtained from the Takano Formation, Central Japan. *Quat. Res.* 46, 305–325. doi: 10.4116/jaqua.46.305

Nagahashi, Y., Yoshikawa, S., Miyakawa, C., Uchiyama, T., and Inouchi, Y. (2004). Stratigraphy and chronology of widespread tephra layers during the past 430 ky in Kinki District and the Yatsugatake Mountains: major element composition of the glass shards using EDS analysis. *Quat. Res.* 43, 15–35. doi: 10.4116/jaqua.43.15

Nagaoka, S. (1984). Late Pleistocene tephrochronology in the region from the Osumi Peninsula to the Miyazaki Plain in South Kyushu, Japan. *J. Geography.* 93, 347–370. doi: 10.5026/jgeography.93.6_347

Nakagawa, M., Fujioka, K., Furuta, T., and Koizumi, S. (1994). Volcanic ash layer in the Leg. 127, 128 core from Japan Sea. *Chikyu Monthly* 16, 691–698.

Nakajima, S., and Maeno, F. (2015). What happen during the catastrophic eruption? *Nikkei Sci.* 45, 4, 32–41.

Nakajima, T., Kikkawa, K., Ikehara, K., Katayama, H., Kikawa, E., Joshima, M., et al. (1996). Marine sediments and late Quaternary stratigraphy in the southeastern part of the Japan Sea -concerning the timing of dark layer deposition-. *J. Geol. Soc. Jpn.* 102, 125–138. doi: 10.5575/geosoc.102.125

NEDO (1995). *Report of Geothermal Development and Promotion, Aso Western Region*, 38. Tokyo: New Energy and Industrial Technology Development Organization.

NIED (2020). *Geo Station*. Available online at: http://www.geo-stn.bosai.go.jp/jps/index.html (accessed April 3, 2020)

Okumura, K., Teraoka, Y., Imai, I., Hoshizumi, H., Ono, K., and Shishido, A. (2010). *Geology of the Nobeoka District. Quadrangle Series, 1:50,000*. Tsukuba: Geological Survey of Japan, AIST.

Ono, K. (1965). Geology of the eastern part of Aso Caldera, central Kyushu, Southwest Japan. *J. Geol. Soc. Jpn.* 71, 541–553. doi: 10.5575/geosoc.71.541

Ono, K., Matsumoto, Y., Miyahisa, M., Teraoka, Y., and Kambe, N. (1977). *Geology of the Taketa District. Quadrangle Series, 1:50,000*. Kawasaki: Geological Survey of Japan.

Ono, K., and Soya, T. (1968). Stratigraphy of pyroclastic flows from Aso Caldera (abstract). *J. Geol. Soc. Jpn.* 74:101.

Ono, K., and Watanabe, K. (1983). Aso Caldera. *Chikyu Monthly* 5, 73–82.

Ono, K., and Watanabe, K. (1985). *Geological Map of Aso Volcano, 1:50,000*. Tsukuba: Geological Survey of Japan.

Pyle, D. M. (1989). The thickness, volume and grainsize of tephra fall deposits. *Bull. Volcanol.* 51, 1–15. doi: 10.1007/BF01086757

Pyle, D. M. (1995). Assessment of the minimum volume of tephra fall deposits. *J. Volcanol. Geotherm. Res.* 69, 379–382. doi: 10.1016/0377-0273(95)00038-0

Pyle, D. M. (2000). "Sizes of volcanic eruptions," in *Encyclopedia of Volcanoes*, eds H. Sigurdsson, B. F. Houghton, S. R. McNutt, H. Rymer, and J. Stix (Cambridge, MA: Academic Press), 257–264.

Quane, S. L., and Russell, J. K. (2005). Ranking welding intensity in pyroclastic deposits. *Bull. Volcanol.* 67, 129–143. doi: 10.1007/s00445-004-0367-5

Rampino, M. R., and Self, S. (1982). Historic eruptions of Tambora (1815), Krakatau (1883), and Agung (1963), their stratospheric aerosols, and climate impact. *Quat. Res.* 18, 127–143. doi: 10.1016/0033-5894(82)90065-5

Roche, O., Buesch, D. C., and Valentine, G. A. (2016). Slow-moving and far-travelled dense pyroclastic flows during the Peach Spring super-eruption. *Nat. Commun.* 7:10890. doi: 10.1038/ncomms10890

Saito, M., Miyazaki, K., Toshimitsu, S., and Hoshizumi, H. (2005). *Geology of the Tomochi District. Quadrangle Series, 1:50,000*. Tsukuba: Geological Survey of Japan, AIST.

Shimizu, A., Torii, M., Shiihara, M., and Oda, M. (1997). Age assignment of the bottom of Core KH94-3 LM8 PC5 based upon a volcanic ash layer in its lowest part. *Mem. Fac. Sci. Kumamoto Univ.* 15, 1–7.

Shimoyama, S., Kameyama, T., Miyata, Y., and Tashiro, Y. (1984). The Quaternary formations of Itoshima coastal plain, Fukuoka Prefecture. *J. Fac. Literature Kitakyushu Univ.* Ser. B 17, 39–58.

Smith, V. C., Staff, R. A., Blockley, S. P. E., Bronk Ramsey, C., Nakagawa, T., Mark, D. F., et al. (2013). Project Members (2013). Identification and correlation of visible tephras in the Lake Suigetsu SG06 sedimentary archive, Japan: chronostratigraphic markers for synchronizing of east Asian/west Pacific palaeoclimatic records across the last 150 ka. *Quat. Sci. Rev.* 67, 121–137. doi: 10.1016/j.quascirev.2013.01.026

Sparks, R. S. J., Self, S., and Walker, G. P. L. (1973). Products of ignimbrite eruptions. *Geology* 1, 115–118. doi: 10.1130/0091-7613(1973)1<115:POIE>2.0.CO;2

Sulpizio, R. (2005). Three empirical methods for the calculation of distal volume of tephra-fall deposits. *J. Volcanol. Geotherm. Res.* 145, 315–336. doi: 10.1016/j.jvolgeores.2005.03.001

Suto, S., Inomata, T., Sasaki, H., and Mukoyama, S. (2007). Database of the volcanic ash fall distribution map of Japan. *Bull. Geol. Surv. Jpn.* 58, 261–321. doi: 10.9795/bullgsj.58.261

Suzuki, T. (1970). The relation between porosity and compressive strength in some welded-tuff. *Bull. Volcanol. Soc. Japan* 15, 132–139. doi: 10.18940/kazanc.15.3_132

Suzuki, T., and Ono, K. (1963). Vertical variation of lithologic characters and intensity of natural remanent magnetization of the Aso pyroclastic flow deposit. *Bull. Volcanol. Soc. Japan* 8, 144–150. doi: 10.18940/kazanc.8.3_144

Suzuki-Kamata, K., and Kamata, H. (1990). The proximal facies of the Tosu pyroclastic-flow deposit erupted from Aso caldera, Japan. *Bull. Volcanol.* 52, 325–333. doi: 10.1007/BF00302046

Takarada, S. (2019). Estimation of eruptive volume of the Aso-4, Aira and Toya eruptions. *Program. Abstracts Volcanol. Soc. Jpn* A3–14:46. doi: 10.18940/vsj.2019.0_46

Takarada, S., Kudo, T., Geshi, N., and Hoshizumi, H. (2017). Distribution and eruptive volume estimation of Ito, Hachinohe and Aso4 pyroclastic flow deposits. *Abstract, JpGU-AGU Joint Meeting*. SVC50-18. Japan Geoscience Union.

Takarada, S., Miyagi, I., and Tomiya, A. (2018). Estimation of distributions and eruptive volumes of Toya and Kutcharo pyroclastic flows. *Program. Abstracts Volcanol. Soc. Jpn* B3-24:116. doi: 10.18940/vsj.2018.0_116

Takarada, S., Oikawa, T., Furukawa, R., Hoshizumi, H., Itoh, J., Geshi, N., et al. (2016). Estimation of total discharged mass from the phreatic eruption of Ontake volcano, central Japan, on September 27, 2014. *Earth Planets Space* 68:138. doi: 10.1186/s40623-016-0511-4

Takarada, S., Yoshimoto, M., Kitagawa, J., Hiraga, M., Yamamoto, T., Kawanabe, Y., et al. (2001). Volcanic ash falls from the Usu 2000 eruption and situation at the source area. *Bull. Geol. Surv. Jpn.* 52, 167–179. doi: 10.9795/bullgsj.52.167

Takemura, K., and Yokoyama, T. (1989). Sedimentary environments inferred from lithofacies of the Lake Biwa 1400 m core sample, Japan. *Jpn. J. Limnol.* 50, 247–254. doi: 10.3739/rikusui.50.247

Tomiya, A., and Miyagi, I. (2020). Age of the Toya eruption. *Bull. Volcanol. Soc. Jpn.* 65, 13–18. doi: 10.18940/kazan.65.1_13

Trenberth, K. E., and Dai, A. (2007). Effects of Mount Pinatubo volcanic eruption on the hydrological cycle as an analog of geoengineering. *Geophys. Res. Letter.* 34:L15702. doi: 10.1029/2007GL030524

Tsuji, T., Ikeda, M., Furusawa, A., Nakamura, C., Ichikawa, K., Yanagida, M., et al. (2018). High resolution record of Quaternary explosive volcanism recorded in fluvio-lacustrine sediments of the Uwa basin, southwest Japan. *Quat. Int.* 471, 278–297. doi: 10.1016/j.quaint.2017.10.016

Urai, M., and Tsu, H. (1986). *Petro-Magnetic Properties in the Hohi Geothermal Region. Report of Geothermal Resources Assessments Technologies in Japan*. Tsukuba: Geological Survey of Japan, 177–225.

Ushioda, M., Miyagi, I., Suzuki, T., Takahashi, E., and Hoshizumi, H. (2020). Preeruptive P-T conditions and H_2O concentration of the Aso-4 silicic end-member magma based on high-pressure experiments. *J. Geophys. Res. Solid Earth* 125:e2019JB018481. doi: 10.1029/2019JB018481

Vandergoes, M. J., Hogg, A. G., Lowe, D. J., Newnham, R. M., Denton, G. H., Southon, J., et al. (2013). A revised age for the Kawakawa/Oruanui tephra, a key marker for the last glacial maximum in New Zealand. *Quat. Sci. Rev.* 74, 195–201. doi: 10.1016/j.quascirev.2012.11.006

Walker, G. P. L. (1980). The Taupo Pumice: product of the most powerful known (ultraplinian) eruption? *J. Volcanol. Geotherm. Res.* 8, 69–94. doi: 10.1016/0377-0273(80)90008-6

Walker, G. P. L. (1981). An ignimbrite veneer deposit: the trail-maker of a pyroclastic flow. *J. Volcanol. Geotherm. Res.* 9, 409–421. doi: 10.1016/0377-0273(81)90047-0

Watanabe, K. (1972). Geology of the western part of Aso Caldera. *Mem. Fac. Educ. Kumamoto Univ. Nat. Sci.* 21, 75–85.

Watanabe, K. (1978). Studies on the Aso pyroclastic flow deposits in the region to the west of Aso Caldera, Southwest Japan, I: Geology. *Mem. Fac. Educ. Kumamoto Univ. Nat. Sci.* 27, 97–120.

Watanabe, K. (1979). Studies on the Aso pyroclastic flow deposits in the region to the west of Aso Caldera, Southwest Japan, II: Petrology of the Aso-4 pyroclastic flow deposits. *Mem. Fac. Educ. Kumamoto Univ. Nat. Sci.* 28, 75–112.

Watanabe, K. (1986). "Flow and Depositional Mechanism of Tosu Orange Pumice Flow from Aso caldera," in *Research on Characteristic and Disasters of Dry Granular Flow Derived From Volcanic Eruptions. Report of Grant-in-Aid for Research (Natural Disasters) 58020012*, ed. S. Aramaki (Tokyo: Japan Soc. Promotion of Science), 115–128.

Watanabe, K., and Ono, K. (1969). Geology of the vicinity of Omine on the western flank of the Aso caldera. *J. Geol. Soc. Jpn.* 75, 365–374. doi: 10.5575/geosoc.75.365

Wilson, C. J. N. (2001). The 26.5 ka Oruanui eruption, New Zealand: an introduction and overview. *J. Volcanol. Geotherm. Res.* 112, 133–174. doi: 10.1016/S0377-0273(01)00239-6

Wilson, C. J. N., and Walker, G. P. L. (1985). The Taupo eruption, New Zealand I. General aspects. *Phil. Trans. R. Soc. Lond. A.* 314, 199–228. doi: 10.1098/rsta.1985.0019

Yamaguchi, H., Oguchi, C., Nishiyama, K., and Matsukura, Y. (2000). A preliminary report on rock properties of Aso pyroclastic flow deposits. *Bull. Terrestrial Environment Research Center, Tsukuba Univ.* 1, 59–65. doi: 10.15068/00146899

Yamamoto, J. K. (2000). An alternative measure of the reliability of ordinary kriging estimates. *Math. Geol.* 32, 489–509. doi: 10.1023/A:1007577916868

Yamamoto, T. (2015). "Cumulative volume step-diagrams for eruptive magma from major Quaternary volcanoes in Japan," in *GSJ Open-File Report*. Tsukuba: Geological Survey of Japan, AIST, 613.

Yamamoto, T. (2017). Quantitative eruption history of Pleistocene Daisen volcano, SW Japan. *Bull. Geol. Surv. Jpn.* 68, 1–16. doi: 10.9795/bullgsj.68.1

Yoshikawa, S., and Kuwae, M. (2001). Last 400 ka high-resolution volcanic ash chronology from lake sediments in Lake Biwa. *Chikyu Monthly* 23, 594–599.

Conflict of Interest: The authors declare that the research was conducted in the absence of any commercial or financial relationships that could be construed as a potential conflict of interest.